

Resolving the mystery of the dwarf galaxy HIZSS003

Ayesha Begum^{1*}, Jayaram N. Chengalur¹, I. D. Karachentsev² and M. E. Sharina²

¹National Centre for Radio Astrophysics, Post Bag 3, Ganeshkhind, Pune 411 007, India

²Special Astrophysical Observatory, Nizhnii Arkhys 369167, Russia

ABSTRACT

The nearby galaxy HIZSS003 was recently discovered during a blind HI survey of the zone of avoidance (Henning et al. 2000). Follow up VLA as well as optical and near-IR imaging and spectroscopy (Massey et al. 2003; Silva et al. 2005) confirm that it is a low metallicity dwarf irregular galaxy. However there were two puzzling aspects of the observations, (i) current star formation, as traced by H α emission, is confined to a small region at the edge of the VLA HI image and (ii) the metallicity of the older RGB stars is higher than that of the gas in HII region. We present high spatial and velocity resolution Giant Meterwave Radio Telescope (GMRT) observations that resolve these puzzles by showing that HIZSS003 is actually a galaxy pair and that the HII region lies at the center of a much smaller companion galaxy (HIZSS003B) to the main galaxy (HIZSS003A). The HI emission from these two galaxies overlaps in projection, but can be separated in velocity space. HIZSS003B has an HI mass of $2.6 \times 10^6 M_{\odot}$, and a highly disturbed velocity field. Since the velocity field is disturbed, an accurate rotation curve cannot be derived, however, the indicative dynamical mass is $\sim 5 \times 10^7 M_{\odot}$. For the bigger galaxy HIZSS003A we derive an HI mass of $1.4 \times 10^7 M_{\odot}$. The velocity field of this galaxy is quite regular and from its rotation curve we derive a total dynamical mass of $\sim 6.5 \times 10^8 M_{\odot}$.

Key words: galaxies: dwarf – galaxies: kinematics and dynamics – galaxies: individual: HIZSS003 radio lines: galaxies

1 INTRODUCTION

The galaxy HIZSS003 was discovered in the course of a blind HI 21cm survey of the Zone of Avoidance (ZOA) (Henning et al. 1998, Henning et al. 2000). Its very low galactic latitude ($b=0.09^{\circ}$) made identification of the optical counterpart in the Palomar Sky Survey images difficult; however, the HI properties derived from the single dish data were consistent with it being a dwarf irregular galaxy. This was later confirmed by follow-up VLA D array and optical observations (Massey et al., 2003). The VLA map showed two peaks in the HI distribution, a resolved peak at the center of the galaxy and an unresolved secondary peak close to the edge of the HI distribution. While broadband BVRI imaging failed to detect any stars in the galaxy, narrowband H α imaging detected an HII region spatially coincident with the unresolved secondary HI peak in the VLA map. Spectroscopy of the HII region confirmed that its radial velocity agreed with that of the HI emission. Although the identification of an HII region strengthens the conclusion that HIZSS003 is a dwarf irregular galaxy, it is puzzling that the current star formation should be concentrated at the edge of the HI disk. VLT near-IR images as well as MMT spectroscopic data of the HII region were

presented by Silva et al. (2005). The near-IR images revealed a resolved stellar population and allowed the distance to the galaxy to be derived based on the K magnitude of the tip of the red giant branch (TRGB). The derived distance of 1.69 ± 0.07 Mpc agrees well with the previous estimate of 1.8 Mpc by Massey et al. (2003) (based on the assumption that HIZSS003 has zero peculiar velocity with respect to the local group centroid).

From their spectroscopic data Silva et al. (2005) estimate the metallicity ($[O/H]$) of the HII region in HIZSS003 to be ~ -0.9 , comparable to that of other nearby metal poor irregular galaxies. On the other hand, the metallicity ($[Fe/H]$) of the RGB stars (as derived from their colours) is somewhat higher, viz. -0.5 ± 0.1 . That the older RGB stars in the galaxy are more metal rich than the gas associated with on going star formation in the HII region is puzzling. Silva et al. (2005) speculate that the lower metallicity of the HII region is caused by low metallicity gas that is falling into HIZSS003 for the first time. Here we present high resolution GMRT HI images of HIZSS003, which resolve the puzzles of the HII region location and metallicity by showing that HIZSS003 is in fact a galaxy pair, with the HII region being located at the center of a much smaller companion to the main galaxy. Throughout this paper we adopt the Silva et al. (2005) TRGB distance estimate of 1.69 Mpc for HIZSS003.

* E-mail:ayesha@ncra.tifr.res.in

2 OBSERVATIONS AND DATA ANALYSIS

The GMRT (Swarup et al. 1991) observations of HIZSS003 (RA (2000): $07^h00^m29.3^s$, DEC(2000): $-04^\circ12'30''$) were conducted on 23 Aug 2004. An observing bandwidth of 1 MHz centered at 1419.1 MHz (which corresponds to a heliocentric velocity of 290 km s^{-1}) was used. The band was divided into 128 spectral channels, giving a channel spacing of 1.65 km s^{-1} . Flux calibration was done using scans on the standard calibrators 3C147 and 3C286, which were observed at the start and end of the observing run. Phase calibration was done using 0744-064, which was observed once every 40 minutes. Bandpass calibration was done in the standard way using 3C286. The total on-source time was ~ 4 hours.

The data was reduced using standard tasks in classic AIPS. The GMRT has a hybrid configuration which simultaneously provides both high angular resolution ($\sim 2''$ if one uses baselines between the arm antennas) as well as sensitivity to extended emission (from baselines between the antennas in the central array). Data cubes were therefore made at various resolutions including $42'' \times 39''$, $28'' \times 26''$, $23'' \times 18''$, $18'' \times 11''$, $8'' \times 6''$ and $4'' \times 3''$, using uniform weighting. RMS noise per channel for these resolutions is 2.2 mJy, 2.0 mJy, 1.8 mJy, 1.6 mJy and 1.2 mJy respectively. All the data cubes, except $8'' \times 6''$ and $4'' \times 3''$, were deconvolved using the task IMAGR. For the two highest resolution data cubes, the signal to noise ratio was too low for CLEAN to work reliably. A continuum image was made using the average of the line free channels. No continuum was detected from the galaxy to a 3σ flux limit of 1.0 mJy/beam (for a beam size of $28'' \times 26''$). A high resolution continuum map ($4'' \times 3''$ resolution) was also made to search for any compact continuum sources. The only continuum source of note detected is NVSS J070023-041255. The HI column density (as derived from the $42'' \times 39''$ resolution image) along the line of sight to this source is $5.7 \times 10^{20} \text{ atoms cm}^{-2}$. A search for HI absorption, in the direction of this source, gave negative results at all resolutions. The implied lower limit on the spin temperature of the gas (assuming a velocity width of 10 km s^{-1}) is 723 K. For reference we note that NVSS J070023-041255 lies towards the source that we call HIZSS003B below, and that it is close to, but not coincident with the HII region detected by Massey et al. (2003). It appears likely that it is a background source, with no connection to the HI emission. The continuum source was subtracted using the task UVSUB.

3 RESULTS AND DISCUSSION

Channel maps of the HI emission at a resolution of $42'' \times 39''$ are shown in Fig. 1. HI emission is spread over 63 channels and consists of two distinct sources, one spanning 59 channels and the other spanning 26 channels. At this spatial resolution some channels show HI emission connecting the two sources, however it is not clear whether this is due to beam smearing. A HI feature connecting the two sources is also seen in $28'' \times 26''$ and $23'' \times 18''$ resolution data cubes. However, at higher resolutions no such connecting emission is seen in the channel maps. Further, as discussed in more detail below, the velocity field of the bigger source does not appear to be particularly disturbed, and neither source shows signs of two armed tidal distortions. It is possible that the connecting emission seen in Fig. 1 is due to beam smearing. In order to disentangle the HI emission one spectral cube was made for each galaxy in which emission from the other galaxy was blanked out. In the case of channel maps which showed connecting HI, the blanking was

done midway between the two sources. The Fig. 2[A]&[B] show HI images of the two sources at $23'' \times 18''$ resolution made from these blanked cubes. In the rest of the paper, we refer to the the bigger (eastern) galaxy as HIZSS003A and the smaller (western) one as HIZSS003B. The entire HI distribution will be referred as the ‘‘HIZSS003 system’’. The sources HIZSS003A and HIZSS003B correspond to the main HI peak and the secondary unresolved peak in the VLA map of Massey et al. (2003). The combination of poor spatial ($\sim 60''$) and velocity ($\sim 10 \text{ km s}^{-1}$) resolution of the VLA observations prevented Massey et al. (2003) from separating the two galaxies, although the near-IR VLT images do show two separate stellar concentrations, i.e. one for each galaxy. Fig. 2[C] shows the high resolution HI map ($8'' \times 6''$ resolution) of HIZSS003. The more diffuse emission is resolved out, and the remaining emission from the two galaxies can be disentangled without having to resort to channel by channel blanking. As can be seen in the Fig. 2, the HI distribution in both the galaxies is clumpy, with three main peaks seen in the HI distribution of HIZSS003A, whereas the HI distribution of HIZSS003B is resolved into two peaks. No signature of tidal interaction is evident in the HI distribution of either galaxy. The HII region detected in the HIZSS003 system is located close to one of the peaks of the HI distribution in HIZSS003B (shown by a cross in Fig. 2[C]). The $\text{H}\alpha$ emission is approximately aligned with the HI contours of the galaxy (i.e. from northwest to southeast), and its heliocentric velocity ($335 \pm 15 \text{ km s}^{-1}$ – Massey et al. 2003), matches within the error bars with the systemic velocity of $322.6 \pm 1.4 \text{ km s}^{-1}$ for HIZSS003B derived from the HI global profile (see below).

Fig. 3 shows the global HI emission profiles of the two galaxies obtained from the $42'' \times 39''$ resolution data cubes. As discussed above, emission from one galaxy was blanked before obtaining the HI profile for the other one. Gaussian fits to the HI profiles give systemic velocities of $288.0 \pm 2.5 \text{ km s}^{-1}$ and $322.6 \pm 1.4 \text{ km s}^{-1}$ for HIZSS003A and HIZSS003B respectively. The corresponding velocity widths at 50% of peak emission are 55 km s^{-1} and 28 km s^{-1} , while the integrated fluxes are $20.9 \pm 2.1 \text{ Jy km s}^{-1}$ and $3.8 \pm 0.3 \text{ Jy km s}^{-1}$. The HI masses corresponding to these integrated fluxes are $1.4 \times 10^7 M_\odot$ and $2.6 \times 10^6 M_\odot$. The combined flux of both galaxies is $24.7 \text{ Jy km s}^{-1}$, which is in excellent agreement with the value of $24.9 \text{ Jy km s}^{-1}$ obtained from the VLA observations by Massey et al. (2003). However both these values are somewhat lower than the flux integral of $\sim 32 \text{ Jy km s}^{-1}$, estimated from the single dish observations by Henning et al. (2000). The HI diameter of the two galaxies, measured at a level of $\sim 10^{19} \text{ atoms cm}^{-2}$ (from the $42'' \times 39''$ images) are $\sim 6.5'$ (3.2 kpc) and $\sim 3'$ (1.5 kpc).

Fig. 4[A]&[B] show the velocity fields of the two galaxies derived from the moment analysis of $28'' \times 26''$ resolution data cube. The velocity field of HIZSS003A (Fig. 4[A]) is regular and a large scale velocity gradient, consistent with systematic rotation, is seen across the galaxy. The velocity field is also mildly lopsided – the isovelocity contours in the southern half of the galaxy are more curved than the northern half. Kinks are seen in the eastern isovelocity contours, close to the location of HIZSS003B. These kinks are more prominent in the higher resolution velocity fields (not shown).

Rotation curves of HIZSS003A were derived using $42'' \times 39''$, $28'' \times 26''$, $23'' \times 18''$ and $18'' \times 11''$ resolution velocity fields, using tilted ring fits. The center and systemic velocity for the galaxy obtained from a global fit to the various resolution velocity fields matched within the error bars; the systemic velocity of 291.0 ± 1.0

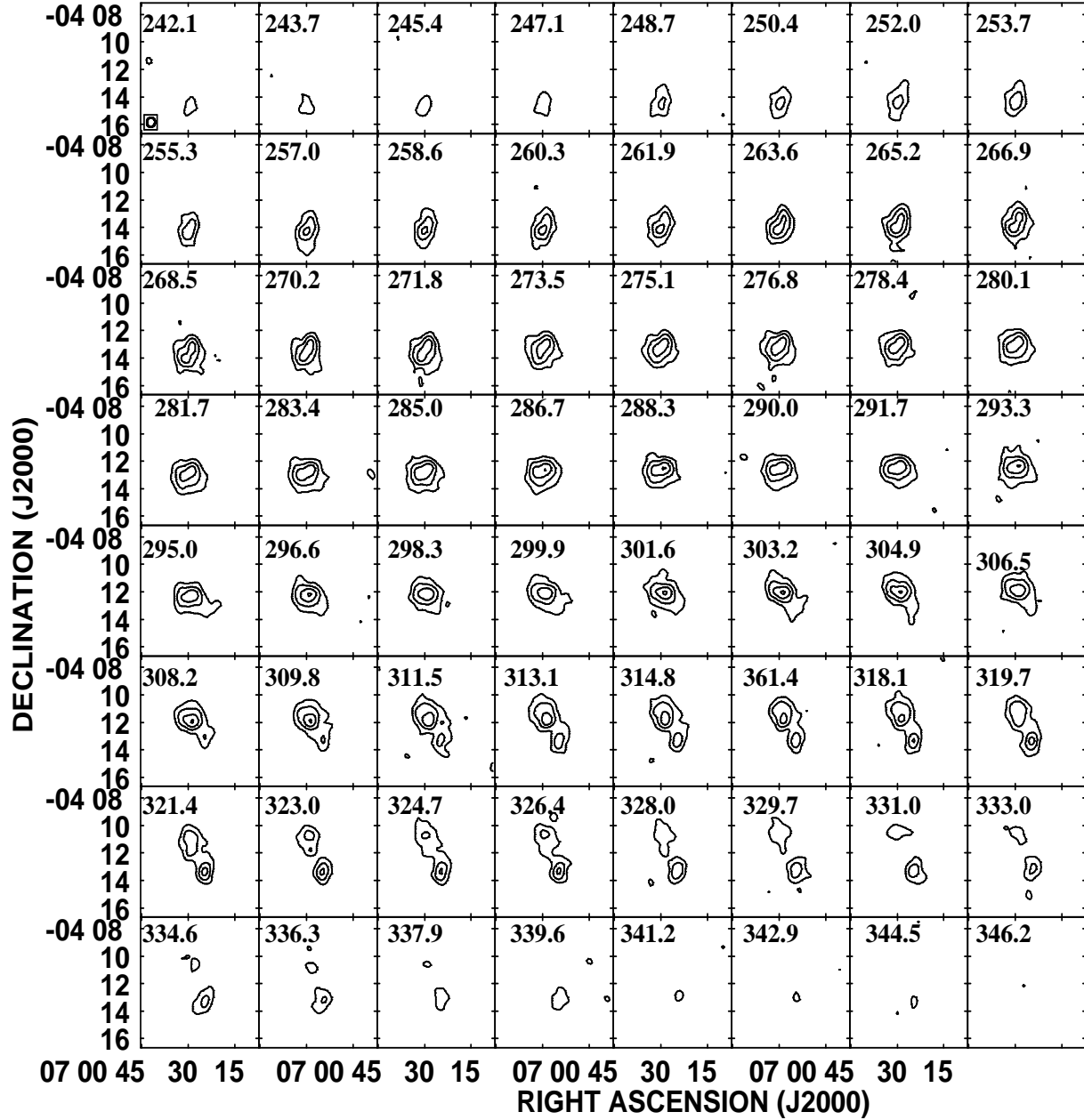


Figure 1. HI channel maps of HIZSS003 at $42'' \times 39''$ resolution. The contour levels are 7.5, 22.5, 45 and 75 mJy km s^{-1} . The heliocentric velocity in km s^{-1} is marked on the upper left-hand corner of every pane. The channel spacing is 1.65 km s^{-1} .

km s^{-1} also matched with the value obtained from the global HI profile of the galaxy. Keeping the center and systemic velocity fixed, we fitted for the inclination and position angle (PA) in each ring. For all resolution velocity fields, the PA was found to vary from $\sim -4^\circ$ to 4° and the inclination varied from $\sim 70^\circ$ to 55° . Keeping the PA and inclination fixed to 3° and 65° in the inner regions (upto $90''$) and 0° and 60° in the outer regions respectively, the rotation curves at various resolutions were derived. Fig. 4[C]

shows the rotation curve of the galaxy derived at various resolutions – as can be seen, they match within the errorbars. The solid line show the final adopted rotation curve. The total dynamical mass of HIZSS003A (at the last measured point of the rotation curve) is found to be $6.5 \times 10^8 M_\odot$.

The velocity field of HIZSS003B (Fig. 4[B]) shows a large scale gradient in the southeast-northwest direction with a magnitude of $\sim 5 \text{ km s}^{-1} \text{ kpc}^{-1}$. This gradient is aligned along the direc-

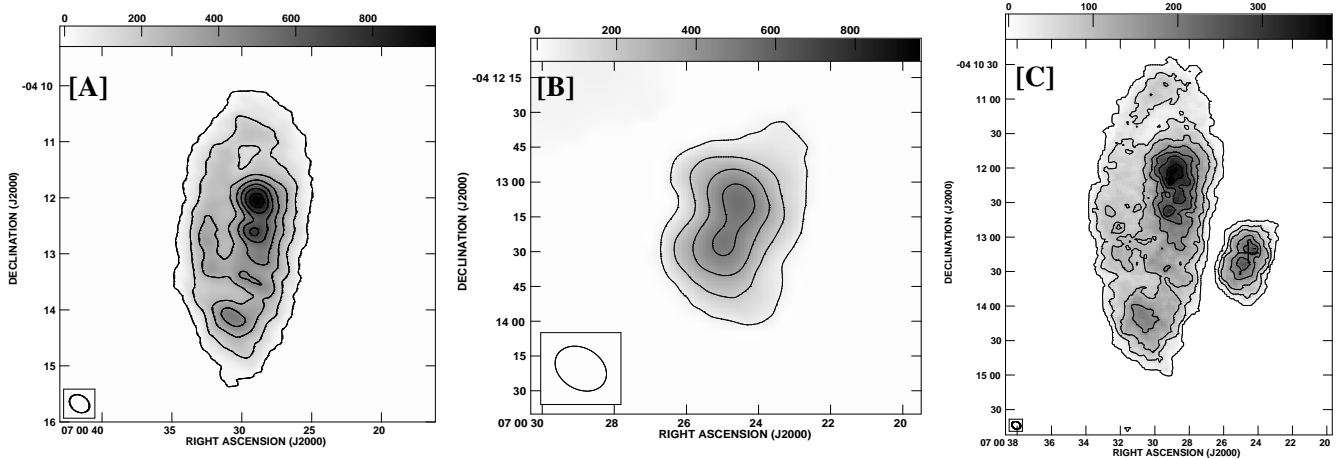


Figure 2. Integrated HI emission maps (grey scales and contours) of HIZSS003A (panel [A]) and HIZSS003B (panel [B]) at $23'' \times 18''$ resolution. The contour levels are 0.2, 3.9, 7.8, 11.6, 15.4, 19.1, 31.4 and 24.9×10^{20} atoms cm^{-2} . The angular scale for panel [B] has been expanded for clarity. [C] Integrated HI emission map of HIZSS003 system (grey scale and contours) at $8'' \times 6''$ resolution. The contour levels are 0.03, 0.05, 0.10, 0.17, 0.21, 0.27, 0.34 and $0.36 \text{ Jy/beam km s}^{-1}$. The location of HII region in HIZSS003B is marked by a cross.

tion of elongation of the HI contours and also with the HII region in the galaxy (Fig. 2[B]). However, the observed velocity pattern is clearly not rotation since the velocity gradient is not monotonic. Both ends of the galaxy are at a higher velocity than the central region. Similar kinematics are seen in other very low mass dwarf galaxies e.g. Sag DIG and LGS 3 (Young & Lo 1997). The disturbed kinematics may be due to a combination of tidal perturbation from the companion galaxy and energy input from the ongoing star formation (see e.g. GR8, Begum & Chengalur 2003). The inclination of HIZSS003B derived from the ellipse fit to the HI distribution (assuming an intrinsic axial ratio $q_0=0.25$) is $\sim 50^\circ$, which means that the upper limit to the inclination corrected rotation velocity is $5/\sin(50) \sim 6.5 \text{ km s}^{-1}$. Assuming that the gas has a velocity dispersion (σ) of 8 km s^{-1} , (which is a typical value for low mass dwarf irregular galaxies, e.g. Lake et al. 1990, Begum et al. 2003), implies that the systematic rotation, if any, in the galaxy is smaller than the velocity dispersion. Given the lack of any systematic rotation, it is difficult to accurately determine the total dynamical mass for the galaxy. From the virial theorem, assuming HI distribution to be spherical with an isotropic velocity dispersion and negligible rotation, the indicative mass is (Hoffman et al. 1996)

$$M_{\text{VT}} = \frac{5 r_{\text{H}} \times \sigma^2}{G} \quad (1)$$

Assuming σ of 8 km s^{-1} and taking the diameter of the galaxy $\sim 1.5 \text{ kpc}$, gives a total mass of HIZSS003B to be $\sim 5.3 \times 10^7 M_\odot$. For the entire HIZSS003 system, if we assume the two galaxies to be in a bound circular orbit, then the indicative orbital mass is

$$M_{\text{orb}} = \frac{32}{3\pi G} r_p \Delta V^2 \quad (2)$$

where r_p is the projected separation and ΔV the radial velocity difference (Karachentsev et al. 2002). For a projected separation of $\sim 0.7 \text{ kpc}$ and a velocity difference of $\sim 34.6 \text{ km s}^{-1}$, the indicative orbital mass is $\sim 6.7 \times 10^8 M_\odot$, in good agreement with the total mass derived from the internal kinematics.

Silva et al. (2005) highlight a puzzle regarding the metallicity of HIZSS003. The metallicity of HIZSS003 system calculated

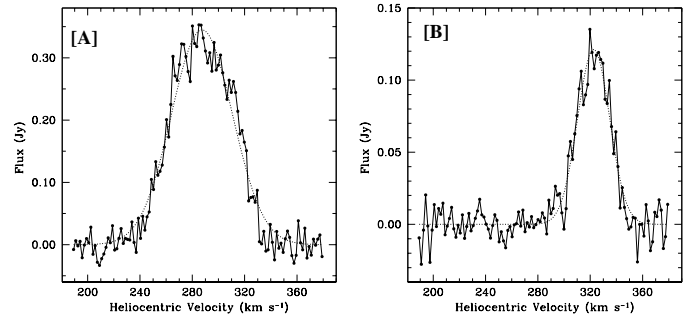


Figure 3. Global HI emission profiles for HIZSS003A (panel [A]) and HIZSS003B (panel [B]) obtained from the $42'' \times 39''$ data cube. The dashed lines show gaussian fits to the profiles.

from the younger HII region is smaller than that estimated from the color of the older red giant branch stars. Given that the bulk of the stars are associated with the bigger galaxy but that the HII region is in the smaller galaxy, the inconsistency in the derived metallicities is not surprising. The low metallicity of the gas in the HII region of the smaller galaxy HIZSS003B is also qualitatively consistent with what one would expect from the metallicity-luminosity relation. Further, going by the stars identified as belonging to the HII region (Fig. 6 of Silva et al. 2005) there is a trend for these stars to have a slightly smaller J-K color (consistent with a lower metallicity; Valenti et al. 2004) than the median color of all stars identified as belonging to HIZSS003. The HIZSS003 puzzle thus seems (at a qualitative level at least) resolved. However, as is well known, an observed colour difference cannot be uniquely ascribed to a difference in the metallicity, but could also be due to a difference in the age of the stars ("age-metallicity" degeneracy) or from a temperature difference. A more quantitative consistency check will have to await a detailed reanalysis of the near-IR data.

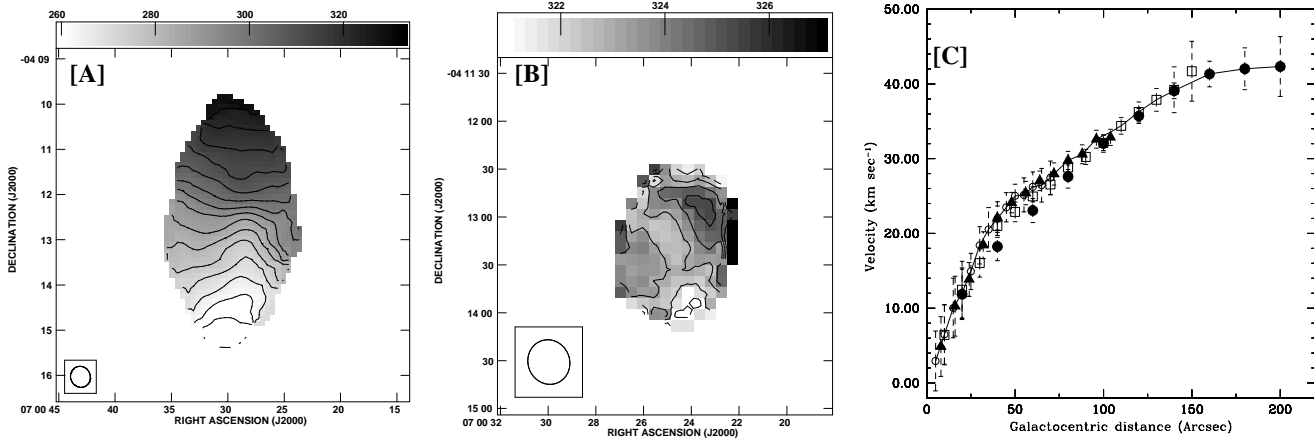


Figure 4. [A]The HI velocity field of HIZSS003A at $28'' \times 26''$ resolution. The contours are in the steps of 5 km s^{-1} and range from 251.0 km s^{-1} to 326.0 km s^{-1} . [B]The HI velocity field of HIZSS003B at $28'' \times 26''$ resolution. The contours are in the steps of 1 km s^{-1} and range from 321.0 km s^{-1} to 326.0 km s^{-1} . The angular scale for this figure has been expanded for clarity. [C]The rotation curve for HIZSS003A derived from the intensity weighted velocity field at $42'' \times 39''$, $28'' \times 26''$, $23'' \times 18''$ and $18'' \times 11''$ resolution (shown as filled circles, open squares, filled triangles and open circles respectively). The solid line shows the adopted rotation curve.

ACKNOWLEDGMENTS

The observations presented in this paper were made with the Giant Metrewave Radio Telescope (GMRT). The GMRT is operated by the National Center for Radio Astrophysics of the Tata Institute of Fundamental Research.

REFERENCES

- Begum, A., Chengalur, J.N. & Hopp, U., 2003, *New Astronomy*, 8, 267
 Begum, A & Chengalur, J.N., 2003, *A&A*, 409, 879
 Henning, P.A., Kraan-Korteweg, R.C., Rivers, A.J., Loan, A.J., Lahav, O. & Burton, W.B., 1998, *AJ*, 115, 584
 Henning, P.A., et al. 2000, *AJ*, 119, 2686
 Hoffman, G.L., Salpeter, E.E., Farhat, B., Roos, T., Williams, H. & Helou, G, 1996, *ApJS*, 105, 269
 Karachentsev et al. 2002, *A&A*, 383, 125
 Lake, G., Schommer, R. A. & van Gorkom, J.H., 1990, *AJ*, 99, 547
 Massey, P., Henning, P.A. & Kraan-Korteweg, R.C., 2003, *AJ*, 126, 2362.
 Silva, D.R., Massey, P., DeGioia-Eastwood, K. & Henning, P.A., 2005, *ApJ*, 623
 Swarup, G., Ananthakrishnan, S., Kapahi, V.K., Rao, A.P., Subrahmanya, C.R. & Kulkarni, V.K. 1991, *Current Science*, 60, 95
 Valenti, E., Ferraro, F.R. & Origlia, L., 2004, *MNRAS*, 351, 1204
 Young, L.M. & Lo, K.Y., 1997, *ApJ*, 490, 710